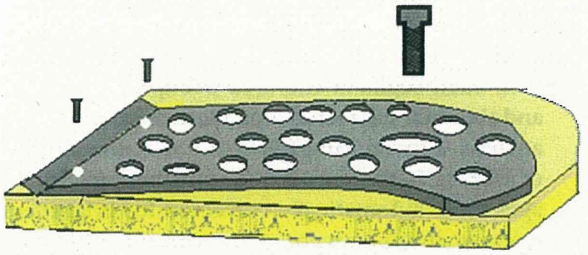

FIGURE 3. Device and position of fixation and elevation screws.

Zakaria, Madi, and Kasugai. Induced Osteogenesis by Periosteal Distractor. J Oral Maxillofac Surg 2012.

incision was performed over the calvarial bone. The skin and periosteal flap were carefully raised to expose the bone surface, and then the periosteum was retracted away from the operative site. Under irrigation with saline solution, 2 or 3 perforations were made with a No. 4 round bur to expose the modular cavity in the external cortical layer of the occipital bone. This exposure acted as an active source for osteoblast progenitor cells in the site during distraction. The mesh was first placed over the perforated area and then fixed to the bone surface from one end by means of 2 micro-screws (Fig 4). The periosteum was sutured back in place, covering the whole mesh (Fig 5). Finally, the skin flaps were sutured with No. 3-0 silk (Ethicon, Somerville, NJ) (Fig 6).

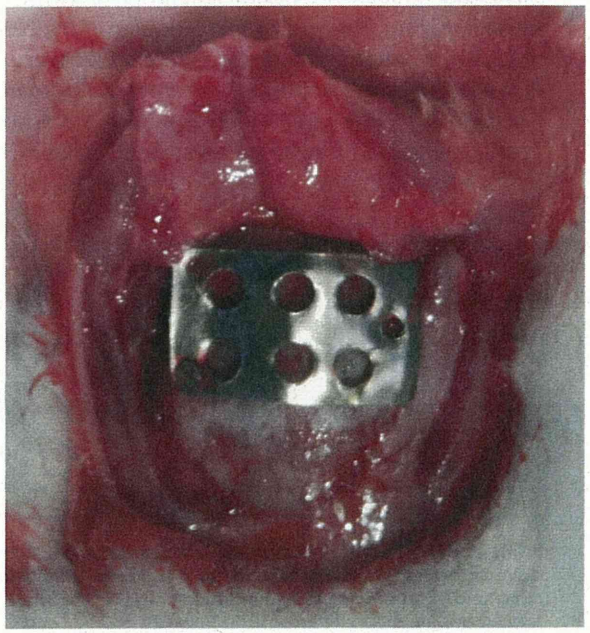

FIGURE 4. Periosteal distractor fixed on calvaria bone.

Zakaria, Madi, and Kasugai. Induced Osteogenesis by Periosteal Distractor. J Oral Maxillofac Surg 2012.

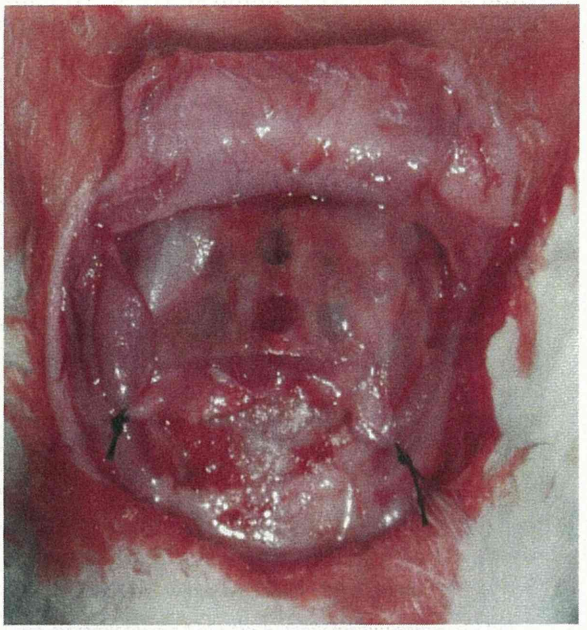

FIGURE 5. Distractor covered by periosteum.

Zakaria, Madi, and Kasugai. Induced Osteogenesis by Periosteal Distractor. J Oral Maxillofac Surg 2012.

Device Activation

In groups 1 and 2, at 1 week after device placement, a soft tissue incision of 2 mm in length was made over the screw hole in the mesh. The elevation screw was threaded through the mesh to raise it. The

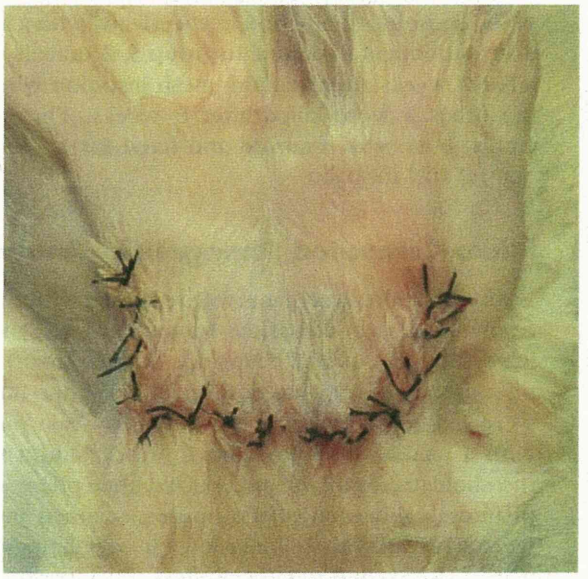

FIGURE 6. Flap closure.

Zakaria, Madi, and Kasugai. Induced Osteogenesis by Periosteal Distractor. J Oral Maxillofac Surg 2012.

FIGURE 7. Elevation screw insertion.

Zakaria, Madi, and Kasugai. Induced Osteogenesis by Periosteal Distractor. J Oral Maxillofac Surg 2012.

rotating screw perforated the covering soft tissue and was resting on the external cortical layer of the calvarial bone (Fig 7). Rotating the screw 180° caused the titanium mesh to be elevated by 0.5 mm. A rate of 0.5 mm of distraction was applied twice a day for 5 days. Group 3 (control group) animals received no elevation screw, and, hence, devices were not activated.

During the observation period, all rabbits were given water and standard rabbit feed ad libitum. Group 1 and 2 animals were killed after 4 and 6 weeks of the consolidation period, respectively, with a lethal dose of thiopental sodium. In group 3, 2 animals were killed 4 weeks after titanium mesh insertion whereas the other 2 were killed after 6 weeks. The entire cranial bone was removed and fixed for 14 days in neutral 10% formalin.

Micro-Computed Tomography Analysis

After fixation, specimens were scanned with a high-resolution micro-computed tomography (CT) imaging system (SMX-90CT; Shimadzu, Kyoto, Japan) continuously in increments of 60 μm. The bone images were extracted by processing the grayscale images with a median filter to remove noise[20] and a fixed threshold to extract the mineralized bone phase. After phantom calibration of the images, scanned images were analyzed with 3-dimensional image analysis software (TRI/3D-BON; Ratoc System Engineering, Tokyo, Japan). We obtained 10 micro-CT serial longitudinal images for each specimen (1 image per millimeter). The distracted area in each image was divided equally into 3 segments by the imaginary lines L1, L2, L3, and L4 (Fig 8).

In each segment the area occupied by new bone and the total distracted area were measured by image analysis software (ImageJ, 1.43 Hz; National Institutes of Health, Bethesda, MD) (Supplementary Fig 1). Images were automatically corrected for brightness and contrast and then were converted into 8-bit grayscale before measurement.[16]

The percentage of the newly formed bone per distracted volume (BV/DV) in each segment was calculated. Table 1 shows the BV/DV means for all segments in the 8 animals representing the 2 experimental groups, including the mean and standard deviation of each segment. Heights attained by the periosteum at the end of activation at the L2 and L3 axis were calculated by rules of a right-angled triangle (Fig 9), and consequently, elevation rates at these points were calculated (Table 2). In the control group specimens were histologically inspected to observe new bone formation over or under the device.

Statistical analysis was performed with the SPSS statistical package (SPSS, Chicago, IL). Descriptive statistics included mean and standard deviation, as well as the 1-way analysis of variance test, to compare the BV/DV ratio in the 3 segments between the 2 groups. The level of significance was set at 95%.

Histologic Processing

After fixation, calvarial bone was dehydrated in ascending grades of ethanol and then embedded in polyester resin (Rigolac-70F and Rigolac-2004; Nisshin EM, Tokyo, Japan). The distraction devices were kept in place, and then sections were cut (Exakt; Mesmer, Ost Einbeck, Germany) and ground to a thickness of about 100 μm. The sections were finally stained with

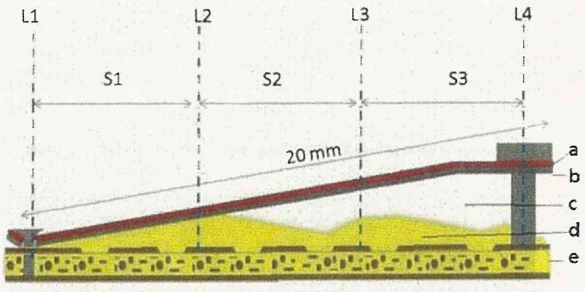

FIGURE 8. Transverse section showing 3 distracted segments: S1, distracted segment close to fixed end; S2, middle distracted segment; and S3, distracted segment close to movable end. L1, L2, L3, and L4 are imaginary lines passing between S1, S2, and S3. (a, periosteum; b, device; c, connective tissue; d, newly formed bone; e, original bone.)

Zakaria, Madi, and Kasugai. Induced Osteogenesis by Periosteal Distractor. J Oral Maxillofac Surg 2012.

Table 1. BV/DV VALUES IN PERCENT

	Group 1			Group 2		
	S1	S2	S3	S1	S2	S3
Rabbit 1	58.9	17.8	23.81	88	40.39	8.28
Rabbit 2	72.48	17.05	13.43	83.84	66.38	17.18
Rabbit 3	85.54	25.8	15.35	90	64.44	16.744
Rabbit 4	85.21	42.55	5.85	87.29	76.16	21.28
Mean	75.53	25.8	14.61	87.28	61.84	15.87
SD	12.64	5.45	7.37	2.56	7.37	5.45

Zakaria, Madi, and Kasugai. Induced Osteogenesis by Periosteal Distractor. J Oral Maxillofac Surg 2012.

0.1% toluidine blue. Histologic observation was performed under a light microscope.

Results

In all animals normal dietary habits were resumed immediately after cessation of the general anesthesia effect. No infections were detected during the entire period of the experiment. All devices remained rigidly fixed to the calvaria during the experiment. They were totally covered by the soft tissue during activation and until time of sacrifice. Distraction screws were easily adjusted and remained attached to the device until the end of the experiment.

At 4 weeks of the consolidation period, on transverse histologic sections, multiple dome-shaped bones outlined by thin bone trabeculae and scattered bone trabeculae within abundant adipose tissue were evident. A layer of connective tissue was covering the newly formed bone layer (Fig 10). At 6 weeks of the consolidation period, transverse sections showed similar histologic patterns; however, bone trabeculae were thicker and adipose tissue was less abundant (Fig 11).

Newly formed bone trabeculae showed different patterns among the distraction segments at 4 and 6 weeks of the consolidation period. Bone trabeculae in segment 1 (S1) at both time points showed a more compact appearance with a marked decrease in adipose tissue (Fig 12). In addition, new bone trabeculae in S1 were likely to interact with the proliferating periosteum through the holes of the titanium mesh (Fig 13). Bone trabeculae in segment 2 (S2) showed a more loose appearance with a thicker overlying connective tissue layer (Fig 10). At 6 weeks of the consolidation period, small bone trabeculae were observed between the periosteum and the titanium mesh near the anchored end in S1 (Fig 14). Segment 3 (S3) showed an almost similar histologic pattern to S2 with a thicker connective tissue layer. At both 4 and 6 weeks of consolidation, S3 was distinguished by regeneration of promoted quality bone with scant adipose tissue over the serrations of the apical 2 mm of the distraction screw (Fig 15).

In group 3 (control) microscopic observation showed the titanium mesh resting on the cortical bone with a small gap in between (Fig 16). A small amount of new bone and connective tissue was observed to fill the gap in all control specimens, whereas diminutive bone was detected over the mesh in 1 specimen of an animal killed after 6 weeks of device insertion (Fig 17).

At 4 and 6 weeks of consolidation, micro-CT 3-dimensional images showed that the new bone was less radiopaque than the original basal bone. Connective tissue appeared as a radiolucent area of considerable thickness in S3 (Figs 18, 19 [arrows]); however, it tapered off from S3 to S1 and almost disappeared in S1 (Figs 18-21).

Quantitative data showed that S1 at both time points contains the highest new bone volume per

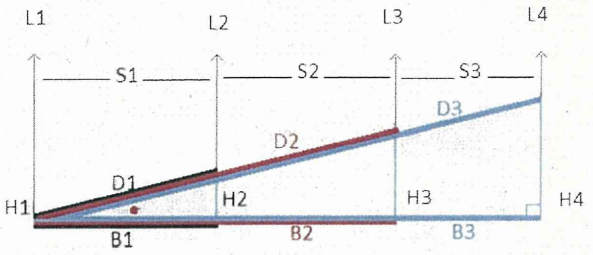

FIGURE 9. Geometric illustration of device and distracted site after full activation. It represents a right angled triangle in which: Red dot is the angle of elevation, L1 and L2 divide the triangle hypotenuse and adjacent sides into 3 equal parts D1, D2 and D3 & B1, B2 and B3. H4(5mm), H3(3.33mm), H2(1.66mm) are the maximum heights of S3, S2, S1 respectively while H1 is minimum height of S1 (0mm).

Zakaria, Madi, and Kasugai. Induced Osteogenesis by Periosteal Distractor. J Oral Maxillofac Surg 2012.

Table 2. ELEVATION RATES IN S1, S2, AND S3

	S1	S2	S3
Elevation rate range (mm/d)	0-0.33	0.33-0.66	0.66-1

Zakaria, Madi, and Kasugai. Induced Osteogenesis by Periosteal Distractor. J Oral Maxillofac Surg 2012.

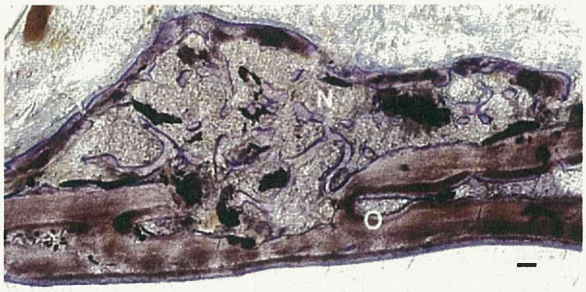

FIGURE 10. Newly formed bone in S2 in group 1. (O, original bone; N, new bone.) (Toluidine blue staining; *scale bar*, 300 μm.)

Zakaria, Madi, and Kasugai. Induced Osteogenesis by Periosteal Distractor. J Oral Maxillofac Surg 2012.

distracted segment volume compared with S2 and S3. The percentage of new bone volume at 6 weeks was higher than that at 4 weeks (Table 1). There were statistical differences between S1 and S2 and between S1 and S3 at 4 weeks. At 6 weeks, there were significant differences between S1 and S3 and between S2 and S3 (Figs 22, 23).

Discussion

The results of this study showed that the new device has effectively induced osteogenesis and successfully distracted the periosteum and overlying soft tissue after 6 weeks in a rabbit calvarial model.

Advantages have been acquired because of the design of the new device. Primarily, it maintained the integrity of the periosteum without interruption. We reported no device displacement, because it was completely hidden under the soft tissues away from the dislodging action of the distracted tissues. Margins of the device were modified to follow the normal contour of the soft tissue when it is activated; hence, no soft tissue dehiscence was reported. Activating the device in an inclined position allowed the application of different distraction speeds to the periosteum simultaneously. The

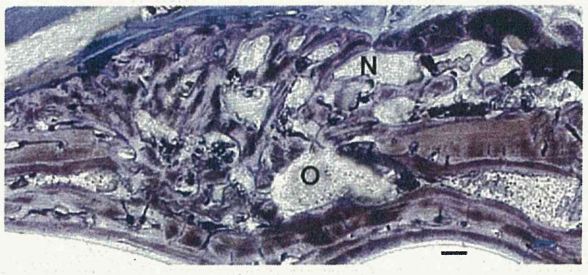

FIGURE 11. Newly formed bone in S2 in group 2. (O, original bone; N, new bone.) (Toluidine blue staining; *scale bar*, 300 μm.)

Zakaria, Madi, and Kasugai. Induced Osteogenesis by Periosteal Distractor. J Oral Maxillofac Surg 2012.

FIGURE 12. Newly formed bone in S1 in group 2 showing more dense trabeculae than in S2. (O, original bone; N, new bone.) (Toluidine blue staining; *scale bar*, 300 μm.)

Zakaria, Madi, and Kasugai. Induced Osteogenesis by Periosteal Distractor. J Oral Maxillofac Surg 2012.

length of the device (20 mm) and its large surface area (200 mm^2) permitted the observation of different bone regeneration patterns in response to different distraction rates.

Sencimen et al[18] and Altuğ et al[19] used the mandible of the rabbit as a model to perform periosteal distraction. They reported an abundance of adipose tissue within the newly formed bone. This was attributed to the distractor design that required incising the periosteum at 3 sites during its application. The device used in our study remarkably preserved the continuity and integrity of the periosteum.

FIGURE 13. Extended bone trabeculae through device perforations and contact with periosteum. (O, original bone; P, periosteum; T, titanium device.) (Toluidine blue staining; *scale bar*, 300 μm.)

Zakaria, Madi, and Kasugai. Induced Osteogenesis by Periosteal Distractor. J Oral Maxillofac Surg 2012.

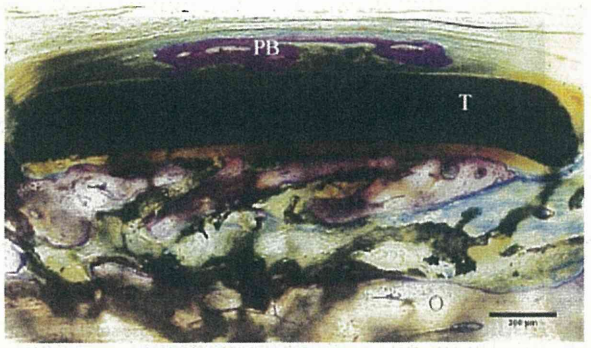

FIGURE 14. Periosteal bone formed over device at S1 in experimental group. (O, original bone; PB, periosteal bone; T, titanium device.) (Toluidine blue staining; *scale bar*, 300 μm.)

Zakaria, Madi, and Kasugai. Induced Osteogenesis by Periosteal Distractor. J Oral Maxillofac Surg 2012.

New bone formed in a supra-osteal manner after raising the periosteum is mainly due to the process of natural bone resorption leading to bone marrow access.[21] Cortical perforation may further ease that access.[16] During periosteal distraction, a competition arises between soft tissue cells derived from periosteum and osteoblast cells originating from cancellous bone in the gradually created space. The former cells have the ability to invade the maintained space and multiply faster than the latter.[21]

In S1 the distance between the mesh and bone surface is compared least with the other segments (Figs 20, 21 [arrows]). This affords a comparatively restricted inlet for soft tissue cells and, consequently, less chance to invade the S1 space. Simultaneously, this gives a better chance for osteoblasts to multiply and occupy the space. This may explain the lesser interference of connective tissue and the high ratio of BV/DV at S1 compared with the other segments (Table 1).

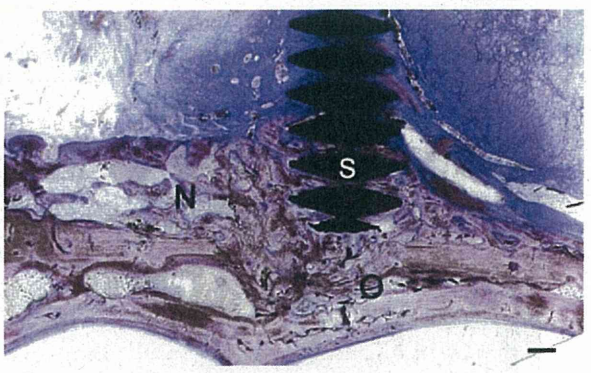

FIGURE 15. New bone trabeculae in S3 creeping over serrations of elevation screw. (O, original bone; N, new bone; S, screw.) (Toluidine blue staining; *scale bar*, 300 μm.)

Zakaria, Madi, and Kasugai. Induced Osteogenesis by Periosteal Distractor. J Oral Maxillofac Surg 2012.

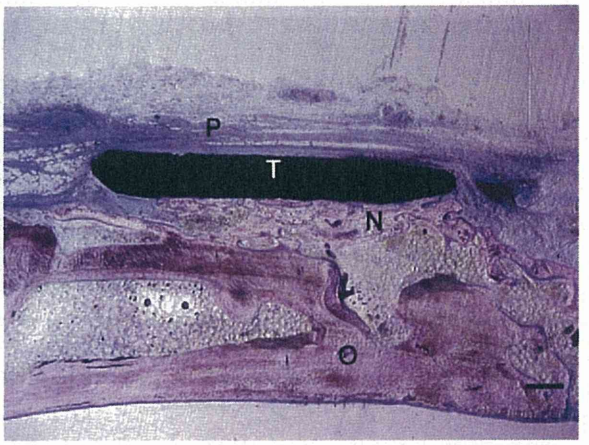

FIGURE 16. New bone filling the minute gap between the original bone surface and the titanium device (control group). (O, original bone; N, new bone; P, periosteum; T, titanium device.) (Toluidine blue staining; *scale bar*, 300 μm.).

Zakaria, Madi, and Kasugai. Induced Osteogenesis by Periosteal Distractor. J Oral Maxillofac Surg 2012.

In S3 the distraction rate showed the highest value among the other segments (0.7-1 mm/d) and the lowest ratio of BV/DV. However, in that segment a large amount of bone was observed covering the apical 2 mm of the elevation screw. This can be attributed to the presence of the titanium screw, which acted as a scaffold for bone regeneration, provided that the underlying cortical bone in this

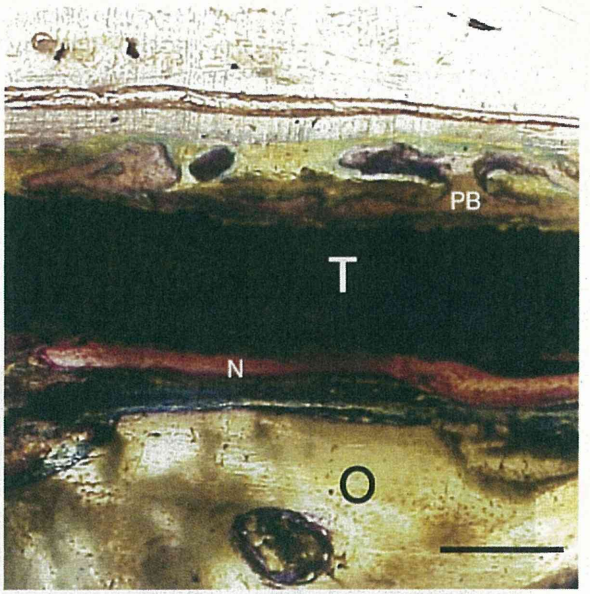

FIGURE 17. Periosteal bone formed over device close to anchored end at 6 weeks in control group. (O, original bone; N, new bone; PB, periosteal bone; T, titanium device.) (Toluidine blue staining; *scale bar*, 300 μm.)

Zakaria, Madi, and Kasugai. Induced Osteogenesis by Periosteal Distractor. J Oral Maxillofac Surg 2012.

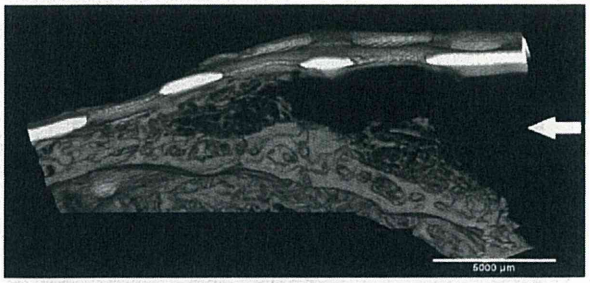

FIGURE 18. Micro-CT image showing transverse view of newly formed bone under device in group 1. *Scale bar,* 5,000 µm.

Zakaria, Madi, and Kasugai. Induced Osteogenesis by Periosteal Distractor. J Oral Maxillofac Surg 2012.

experiment was able to withstand the pressure of the advancing screw (Fig 15).

Altuğ et al[19] claim that lack of bone marrow cells may play a role in the occurrence of fatty tissue; in addition, lack of stimulatory forces may affect the maturity of the newly formed bone. In our study cortical bone perforation was performed to ease access of the bone marrow cells into the distracted site; however, the calvarial bone receives little stimulation, and this may affect the quality of new bone.

On elevation of the periosteum, its osteogenicity starts to be controversial. Some studies claim that it loses its osteogenicity,[22] whereas other studies have indicated that its osteogenic capacity is maintained conditional on contact with bone.[14] Periosteal distraction procedures include separation of periosteum from its underlying bone; however, 3 periosteal distraction studies reported new bone formation near the periosteum.[15,16,23] This was ascribed to the use of an osteoconductive biomaterial as a periosteal distractor. It induced an osteogenic response and promoted new bone formation. In our previous study we performed the same experiment using a device composed of a composite of biodegradable material and micro-hydroxyapatite osteoconductive particles.[16] The amount of new bone formed over and under the

FIGURE 19. Micro-CT image showing transverse view of newly formed bone under device in group 2. *Scale bar,* 5,000 µm.

Zakaria, Madi, and Kasugai. Induced Osteogenesis by Periosteal Distractor. J Oral Maxillofac Surg 2012.

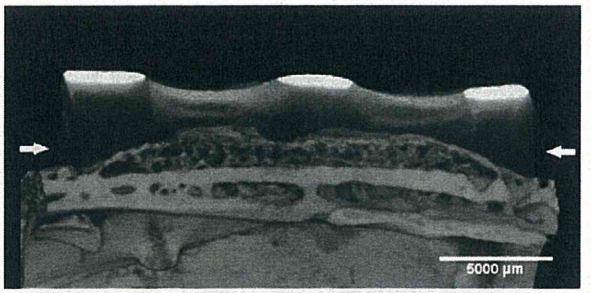

FIGURE 20. Micro-CT image showing cross-sectional view of newly formed bone under device in group 2 in S1. *Scale bar,* 5,000 µm.

Zakaria, Madi, and Kasugai. Induced Osteogenesis by Periosteal Distractor. J Oral Maxillofac Surg 2012.

device was notably higher than that obtained in this experiment. The distractor composition might possibly have affected the induced bone.

The periosteal distraction process involves exerting tension on periosteal tissues. Altering tension of the periosteum may give rise to a stimulatory effect on the cambium cell layer to proliferate and form bone.[24] In distraction osteogenesis, early subperiosteal callus was formed in the gap after osteotomy. This is because the periosteal mesenchymal stem cells received an appropriate level of stimulation and were differentiated into osteoblasts.[25,26] In vitro studies proved that Runx2 and osteogenic factor expression were up-regulated in human periosteal cells upon application of mechanical strain.[27]

However, tension may not solely explain the minute periosteal bone observed in this study because of the presence of other factors. The presence of periosteal bone in the control and experimental groups suggests that it may result from stimulation due to contact with newly formed bone underneath the titanium mesh. The inner layer of periosteum is also a source of bone cells.[28]

Probably, the low distraction speed gave less chance for connective tissue to interfere and more

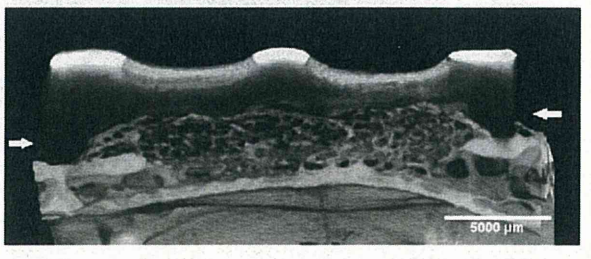

FIGURE 21. Micro-CT image showing cross-sectional view of newly formed bone under device in group 2 in S2. *Scale bar,* 5,000 µm.

Zakaria, Madi, and Kasugai. Induced Osteogenesis by Periosteal Distractor. J Oral Maxillofac Surg 2012.

chances for newly formed bone to interact with proliferating periosteum. During osteogenic distraction, this contact was proven beneficial.[28]

It is reasonable that the optimum osteogenic distraction speed (0.5 to 1 mm/d or more[4,5]) is faster than that suggested in our study. This can be explained because cell and nutrition supplies come from both ends of the bone and the surrounding periosteum in osteogenic distraction; whereas, those supplies originate only from basal bone and periosteum in periosteal distraction.

In previous periosteal distraction studies, the distraction rates varied from 0.2 to 0.5 mm/d.[1,2,8,10,15-19,23] In this study all rates of less than 1 mm/d were included; however, a rate of 0.33 mm/d or less showed the least connective tissue interference. The maximum vertical bone formation, given the distraction rate of 0.33 mm/d in this rabbit model, was 1.49 mm, provided that this new bone height constitutes 90% of the maximum height attained by the device in that segment.

A recent study suggests 0.4 mm/d as an appropriate periosteal distraction rate in a rat calvarial model,[9] which is very close to our value, though applied in a different animal model.

Vertical augmentation of the alveolar bone accompanied by soft tissue expansion is feasible with an osteogenic distractor; however, it is technically sensitive and inconvenient to the patient.[6] Conversely, the device used in this study is compact; thus, it could be more acceptable in the patient's oral cavity.

Lowering the distraction rate seems to be 1 step toward diminution of the connective tissue in the periosteal distraction site. This is in agreement with Ilizarov's principle of tissue distraction that recommended the slow distraction speed of tissues.[29]

However, we recommend that further research should be performed to verify the suggested optimal rate for periosteal distraction using a symmetrically moving device.

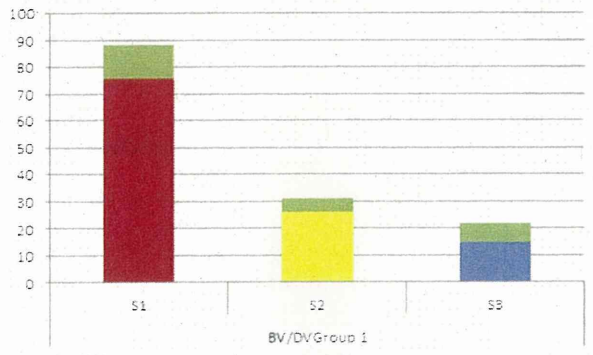

FIGURE 22. Mean and standard deviation of percent of BV/DV among segments in group 1. $P < .01$, Scheffé test.

Zakaria, Madi, and Kasugai. Induced Osteogenesis by Periosteal Distractor. J Oral Maxillofac Surg 2012.

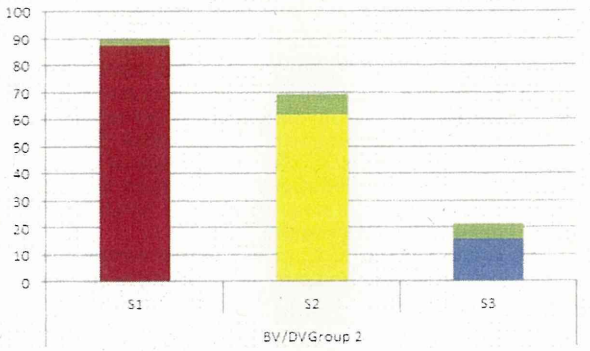

FIGURE 23. Mean and standard deviation of percent of BV/DV among segments in group 2. $P < .01$, Scheffé test.

Zakaria, Madi, and Kasugai. Induced Osteogenesis by Periosteal Distractor. J Oral Maxillofac Surg 2012.

References

1. Schmidt BL, Kung LK, Jones C, et al: Induced osteogenesis by periosteal distraction. J Oral Maxillofac Surg 60:1170, 2002
2. Kessler P, Bumiller L, Schlegel A, et al: Dynamic periosteal elevation. Br J Oral Maxillofac Surg 45:284, 2007
3. Simon MM, Trisi P, Maglione M, et al: A preliminary report on a method for studying the permeability of expanded polytetrafluoroethylene membrane to bacteria in vivo: A scanning electron microscope and histological study. J Periodontol 65:755, 1994
4. Jensen OT, Cockrell R, Kuhike L, et al: Anterior maxillary alveolar distraction osteogenesis: A prospective 5-year clinical study. Int J Oral Maxillofac Implants 17:52, 2002
5. Rachmiel A, Srouji S, Peled M: Alveolar ridge augmentation by distraction osteogenesis. Int J Oral Maxillofac Surg 30:510, 2001
6. Uckan S, Veziroglu F, Dayangac E: Alveolar distraction osteogenesis versus autogenous onlay bone grafting for alveolar ridge augmentation: Technique, complications, and implant survival rates. Oral Surg Oral Med Oral Pathol Oral Radiol Endod 106:511, 2008
7. Chiapasco M, Casentini P, Zaniboni M: Bone augmentation procedures in implant dentistry. Int J Oral Maxillofac Implants 24:237, 2009 (suppl)
8. Estrada JI, Saulacic N, Vazquez L, et al: Periosteal distraction osteogenesis: Preliminary experimental evaluation in rabbits and dogs. Br J Oral Maxillofac Surg 45:402, 2007
9. Saulacic N, Schaller B, Iizuka T, Buser D, Hug C, Bosshardt DD: Analysis of New Bone Formation Induced by Periosteal Distraction in a Rat Calvarium Model. Clin Implant Dent Relat Res. 2011 May 9. doi: 10.1111/j.1708-8208.2011.00355.x. [Epub ahead of print] PMID: 21554531
10. Casap N, Venezia NB, Wilensky A, et al: VEGF facilitates periosteal distraction-induced osteogenesis in rabbits: A microcomputerized tomography study. Tissue Eng Part A 14:247, 2008
11. Bosch C, Melsen B, Vargervik K: Guided bone regeneration in calvarial bone defects using polytetrafluoroethylene membranes. Cleft Palate Craniofac J 32:311, 1995
12. Canalis RF, Burstein FD: Osteogenesis in vascularized periosteum. Interactions with underlying bone. Arch Otolaryngol 111:511, 1985
13. Kostopoulos L, Karring T: Role of periosteum in the formation of jaw bone. An experiment in the rat. J Clin Periodontol 22:247, 1995

14. Kostopoulos L, Karring T, Uraguchi R: Formation of jawbone tuberosities by guided tissue regeneration. An experimental study in the rat. Clin Oral Implants Res 5:245, 1994
15. Yamauchi K, Takahashi T, Funaki K, et al: Periosteal expansion osteogenesis using highly purified beta-tricalcium phosphate blocks: A pilot study in dogs. J Periodontol 79:999, 2008
16. Zakaria O, Kon K, Kasugai S: Evaluation of a biodegradable novel periosteal distractor. J Biomed Mater Res B Appl Biomater. 2011 Oct 13. doi: 10.1002/jbm.b.31944. [Epub ahead of print] PMID: 21998069
17. Oda T, Kinoshita K, Ueda M: Effects of cortical bone perforation on periosteal distraction: An experimental study in the rabbit mandible. J Oral Maxillofac Surg 67:1478, 2009
18. Sencimen M, Aydintug YS, Ortakoglu K, et al: Histomorphometrical analysis of new bone obtained by distraction osteogenesis and osteogenesis by periosteal distraction in rabbits. Int J Oral Maxillofac Surg 36:235, 2007
19. Altuğ HA, Aydintuğ YS, Sençimen M, et al: Oral histomorphometric analysis of different latency periods effect on new bone obtained by periosteal distraction: An experimental study in the rabbit model. Oral Surg Oral Med Oral Pathol Oral Radiol Endod 111:539, 2011
20. Cortical bone analysis, trabecular bone analysis and bone mineral density analysis operation manual. Tokyo: Ratoc System Engineering. April 2008
21. Rompen EH, Biewer R, Vanheusden A, et al: The influence of cortical perforations and of space filling with peripheral blood on the kinetics of guided bone generation. A comparative histometric study in the rat. Clin Oral Implants Res 10:85, 1999
22. Weng D, Hürzeler MB, Quiñones CR, et al: Contribution of the periosteum to bone formation in guided bone regeneration. A study in monkeys. Clin Oral Implants Res 11:546, 2000
23. Yamauchi K, Takahashi T, Funaki K, et al: Histological and histomorphometrical comparative study of β-tricalcium phosphate block grafts and periosteal expansion osteogenesis for alveolar bone augmentation. Int J Oral Maxillofac Surg 39:1000, 2010
24. Simon TM, Van Sickle DC, Kunishima DH, et al: Cambium cell stimulation from surgical release of the periosteum. J Orthop Res 21:470, 2003
25. Delloye C, Delefortrie G, Coutelier L, et al: Bone regenerate formation in cortical bone during distraction lengthening. An experimental study. Clin Orthop Relat Res 34, 1990
26. Hikiji H, Takato T, Matsumoto S, et al: Experimental study of reconstruction of the temporomandibular joint using a bone transport technique. J Oral Maxillofac Surg 58:1270, 2000
27. Kanno T, Takahashi T, Ariyoshi W, et al: Tensile mechanical strain up-regulates Runx2 and osteogenic factor expression in human periosteal cells: Implications for distraction osteogenesis. J Oral Maxillofac Surg 63:499, 2005
28. Takeuchi S, Matsuo A, Chiba H: Beneficial role of periosteum in distraction osteogenesis of mandible: Its preservation prevents the external bone resorption. Tohoku J Exp Med 220:67, 2010
29. Ilizarov GA: The tension-stress effect on the genesis and growth of tissues: Part II. The influence of the rate and frequency of distraction. Clin Orthop Relat Res 263, 1989

APPENDIX SUPPLEMENTARY DATA. Titanium elevation screw length measured using ImageJ software.

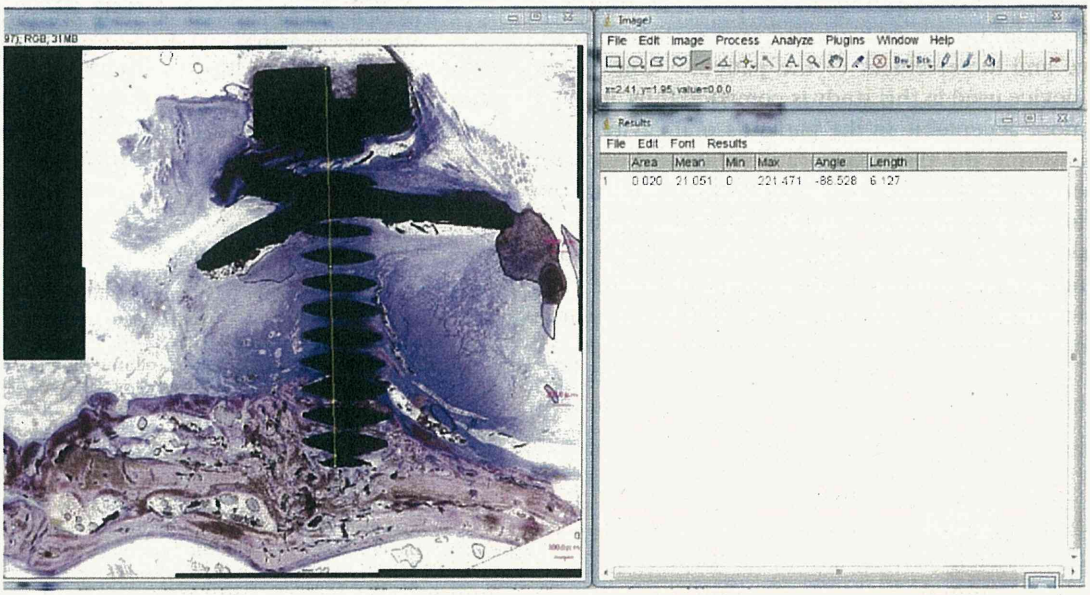

Society For Biomaterials

Evaluation of the osteoconductivity of α-tricalcium phosphate, β-tricalcium phosphate, and hydroxyapatite combined with or without simvastatin in rat calvarial defect

Hisham Rojbani,[1] Myat Nyan,[1] Keiichi Ohya,[2] Shohei Kasugai[1]

[1]Oral Implantology and Regenerative Dental Medicine, Graduate School, Tokyo Medical and Dental University, 1-5-45 Yushima, Bunkyo, Tokyo 113-8549, Japan
[2]Pharmacology, Department of Hard Tissue Engineering, Graduate School, Tokyo Medical and Dental University, Tokyo 113-8549, Japan

Received 7 September 2010; revised 8 January 2011; accepted 17 March 2011
Published online 16 June 2011 in Wiley Online Library (wileyonlinelibrary.com). DOI: 10.1002/jbm.a.33117

Abstract: The purpose of this study is to evaluate the osteoconductivity of three different bone substitute materials: α-tricalcium phosphate (α-TCP), (β-TCP), and hydroxyapatite (HA), combined with or without simvastatin, which is a cholesterol synthesis inhibitor stimulating BMP-2 expression in osteoblasts. We used 72 Wistar rats and prepared two calvarial bone defects of 5 mm diameter in each rat. Defects were filled with the particles of 500–750 μm diameter combined with or without simvastatin at 0.1 mg dose for each defect. In the control group, defects were left empty. Animals were divided into seven groups: α-TCP, β-TCP, HA, α-TCP with simvastatin, β-TCP with simvastatin, HA with simvastatin, and control. The animals were sacrificed at 6 and 8 weeks. The calvariae were dissected out and analyzed with micro CT. The specimens were evaluated histologically and histomorphometrically. In α-TCP group, the amount of newly formed bone was significantly more than both HA and control groups but not significantly yet more than β-TCP group. Degradation of α-TCP was prominent and β-TCP showed slower rate while HA showed the least degradation. Combining the materials with Simvastatin led to increasing in the amount of newly formed bone. These results confirmed that α-TCP, β-TCP, and HA are osteoconductive materials acting as space maintainer for bone formation and that combining these materials with simvastatin stimulates bone regeneration and it also affects degradability of α-TCP and β-TCP. Conclusively, α-TCP has the advantage of higher rate of degradation allowing the more bone formation and combining α-TCP with simvastatin enhances this property. © 2011 Wiley Periodicals, Inc. J Biomed Mater Res Part A: 98A: 488–498, 2011.

Key Words: osteoconductivity, α-tricalcium phosphate, simvastatin, degradation

How to cite this article: Rojbani H, Nyan M, Ohya K, Kasugai S. 2011. Evaluation of the osteoconductivity of α-tricalcium phosphate, β-tricalcium phosphate, and hydroxyapatite combined with or without simvastatin in rat calvarial defect. J Biomed Mater Res Part A 2011:98A:488–498.

INTRODUCTION

The number of clinicians performing endosseous dental implants whether immediately following tooth extraction or after a period of time is rapidly increasing. However, on many occasions clinicians encounter the lack of adequate amount of bone due to a number of reasons including injury, eradicated tumor masses, or progressive periodontal diseases. To overcome this difficulty, many methods have been developed and introduced using a variety of grafts such as autologous bone grafts, allografts, alloplasts, and xenografts.[1] Autologous bone is regarded as one of the gold standard of graft materials.[2–4] However, there are several problems in autologous bone grafts including morbidity of the donor site and limitation of amount of bone that can be harvested.[5,6] It is becoming a demand to identify different types of bone substitutes. Moreover, the process of osteogenesis can be stimulated by applying bone formation stimulating molecules.[7–9] Calcium phosphates, such as tricalcium phosphate (TCP), and hydroxyapatite (HA) are widely used as substitutes for autologous bone.[10,11] These materials show high biocompatibility and osteoconductivity.[12] HA is a biomaterial with a lower degradation rate than new bone formation *in vivo*.[13,14] On the other hand, the degradation rate of TCP is higher than HA *in vivo*. α-TCP dissolves more easily in water than β-TCP even though they have exactly the same chemical composition. However, it is important for a bone substitute material to have the character of degradation rate equal to the process of bone formation.

Interestingly, simvastatin, an inhibitor of cholesterol synthesis, stimulates BMP-2 expression in osteoblasts.[15] We have recently reported that α-TCP containing simvastatin stimulates bone regeneration in rat calvarial defects by enhancing BMP-2 expression.[16] The purpose of this study was to evaluate osteoconductivity of three different calcium phosphate materials, α-TCP, β-TCP, and HA, combined with or without simvastatin in rat calvarial defects.

Correspondence to: H. Rojbani; e-mail: hisham.rojbani@gmail.com

TABLE I. List of the Experimental Groups

Group	Bone Substitute	Simvastatin	Number of Defects
1	α-TCP	−	12
2	α-TCP	+	12
3	β-TCP	−	12
4	β-TCP	+	12
5	HA	−	12
6	HA	+	12
7	Control	−	12

MATERIALS AND METHODS

This study was approved by the institutional committee of animal experiments. Bone substitute particles of α-TCP, β-TCP, and HA of 500–750 μm diameter were kindly supplied by (Advance, Co., Tokyo, Japan). Simvastatin powder (Merck & Co., Whitehouse Station, NJ) was dissolved in ethanol (Wako Pure Chemical Industries, Osaka) and incorporated into each bone substitute particles. The amount of simvastatin in 1 mg bone substitute particles was 7 μg and each calvarial defect received approximately 14 mg bone substitute particles. Thus, finally 0.1 mg simvastatin was applied in each calvarial defect.

Seventy two male Wistar rats (14-week old about 250–350 g) were divided into seven groups, α-tricalcium phosphate (α-TCP), β-tricalcium phosphate (β-TCP), hydroxyapatite (HA), α-TCP with simvastatin, β-TCP with simvastatin, HA with simvastatin, and the control (Table I).

Surgical procedures

The animals were anesthetized with a combination of ketamine (40 mg/kg)–xylazine (5 mg/kg), In addition, 0.2 mL of local anesthetic (2% xylocaine/epinephrine 1:20,000, Fujisawa, Tokyo, Japan) was injected into the surgical sites before the start of surgery. The surgical areas were shaved and disinfected with povidone-iodine (Isodine Surgical Scrub, Meiji, Tokyo, Japan), skin incision, and subperiosteal dissection were carried out, a flap was raised and bone defect of 5 mm diameter was prepared reaching the dura mater of the brain on each side lateral to the sagittal plane with a bone trephine bur. The defects were filled with bone substitute particles according to the group. The control group defects were left unfilled. The periosteoum was repositioned and sutured with a 4-0 Vicryl polyglactin suture (Ethicon, NJ) and the skin was sutured by 4-0 silk (ELP Akiyima Co., Tokyo, Japan) (Fig. 1). The animals were injected subcutaneously for the bone labeling with calcein and tetracycline 7 days and 1 day, respectively, before sacrifice for the histomorphometric analysis. The animals were sacrificed at 6 and 8 weeks after the surgery.

Micro CT and computer analysis

After sacrificing the animals, the calvaria were dissected out and fixed in neutral 10% formalin then examined with soft X-ray radiography and dual-energy X-ray absorptiometry for small animals (DCS-600; Aloka Co., Tokyo). Furthermore micro CT (InspeXio; Shimadzu Science East Corporation, Tokyo) was conducted. Micro CT images were analyzed with Tri/3D-Bone software (RATOC System Engineering Co., Tokyo, Japan). Bone volume (BV), bone mineral contents (BMC), bone mineral density (BMD), and remaining bone substitute particles were measured within the region of interest (ROI).

Histological processing

Specimens were prepared for either paraffin wax embedding for the decalcified sectioning or methyl methacrylate (MMA) embedding for the undecalcified sectioning. Decalcification was carried out by immersing the specimens in 10% EDTA for 4 weeks. Decalcified specimens were dehydrated in ascending

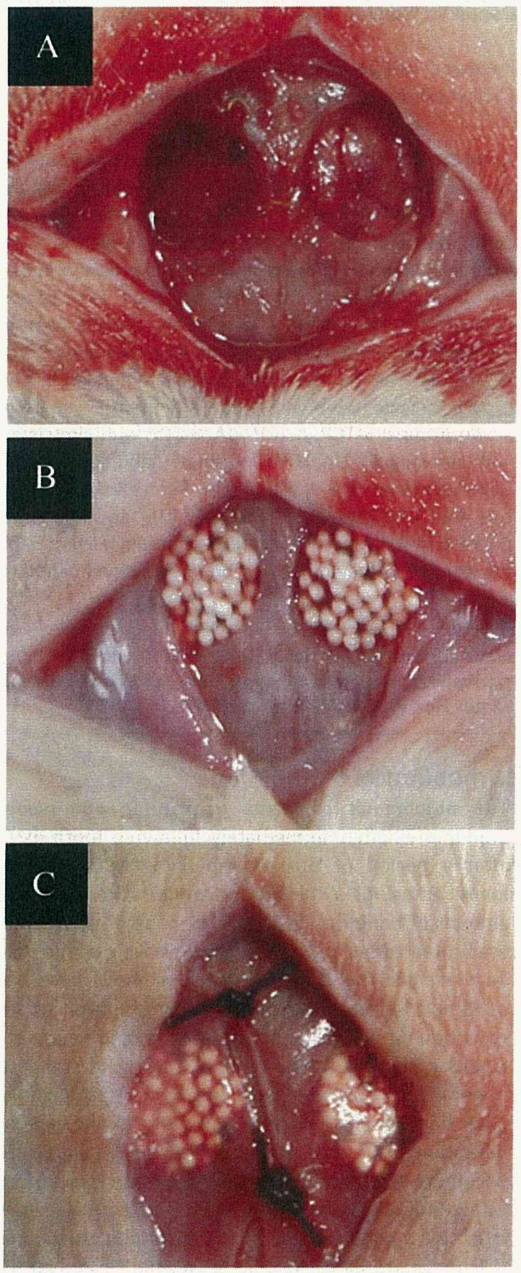

FIGURE 1. Photos of surgical procedures. Subperiosteal dissection (A), bone substitute material applied to the 5 mm defects in the calvarial bone (B), and suturing periosteum with resorbable suture (C).

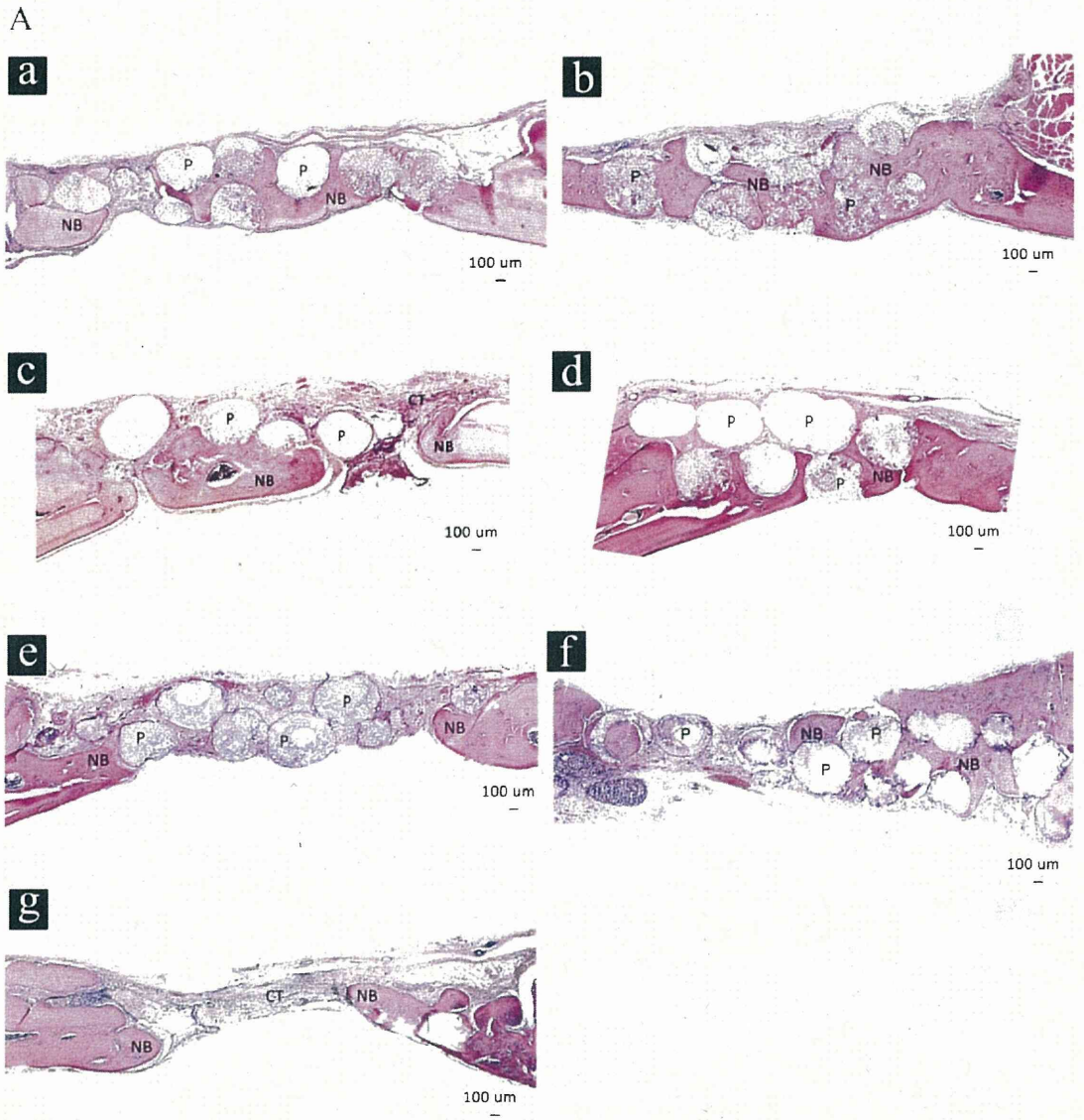

FIGURE 2. (A) Histological images at 6 weeks, α-TCP (a), α-TCP+statin (b), β-TCP (c), β-TCP+statin (d), HA (e), HA+statin (f), and Control (g). Bone substitute particles (P), new bone (NB), and connective tissue (CT). (B) Histological images at 8 weeks. α-TCP (a), α-TCP + statin (b), β-TCP (c), β-TCP + statin (d), HA (e), HA + statin (f), and control (g). Bone substitute particles (P), new bone (NB), and connective tissue (CT). Bone in control group failed to progress toward the center of the defect (g). α-TCP particles were progressively degraded and replaced by new bone (b). [Color figure can be viewed in the online issue, which is available at wileyonlinelibrary.com.]

grades of ethanol and embedded in paraffin wax. Embedded samples were sectioned into 7 μm serial slices with a microtome, following the coronal direction along the defect and calvarial bone. Sections were stained with hematoxylin and eosin.

To obtain undecalcified sections, the specimens were dehydrated in ascending grades of ethanol and acetone and stained with Villanueva bone stain (Wako Pure Chemical Industries, Osaka) for 15 days then infiltrated with and embedded in MMA resin. The MMA embedded sections were cut with a microtome to a thickness about 50 μm following the coronal direction along the defect and calvarial bone.

Histomorphometrical analysis

Both calcified and undecalcified specimens were examined under light microscope (Biozero, BZ-8000; Keyence, Osaka, Japan) for the evaluation of new bone formation among the groups. Fluorescent microscope was used to evaluate the mineral apposition rate (MAR) in the undecalcified samples within one week. Imaging software (ImageJ 1.42q, Wayne Rasband, National Institute of Health) was used to measure the percentage of new bone formation, percentage of remaining bone substitute materials, and MAR.

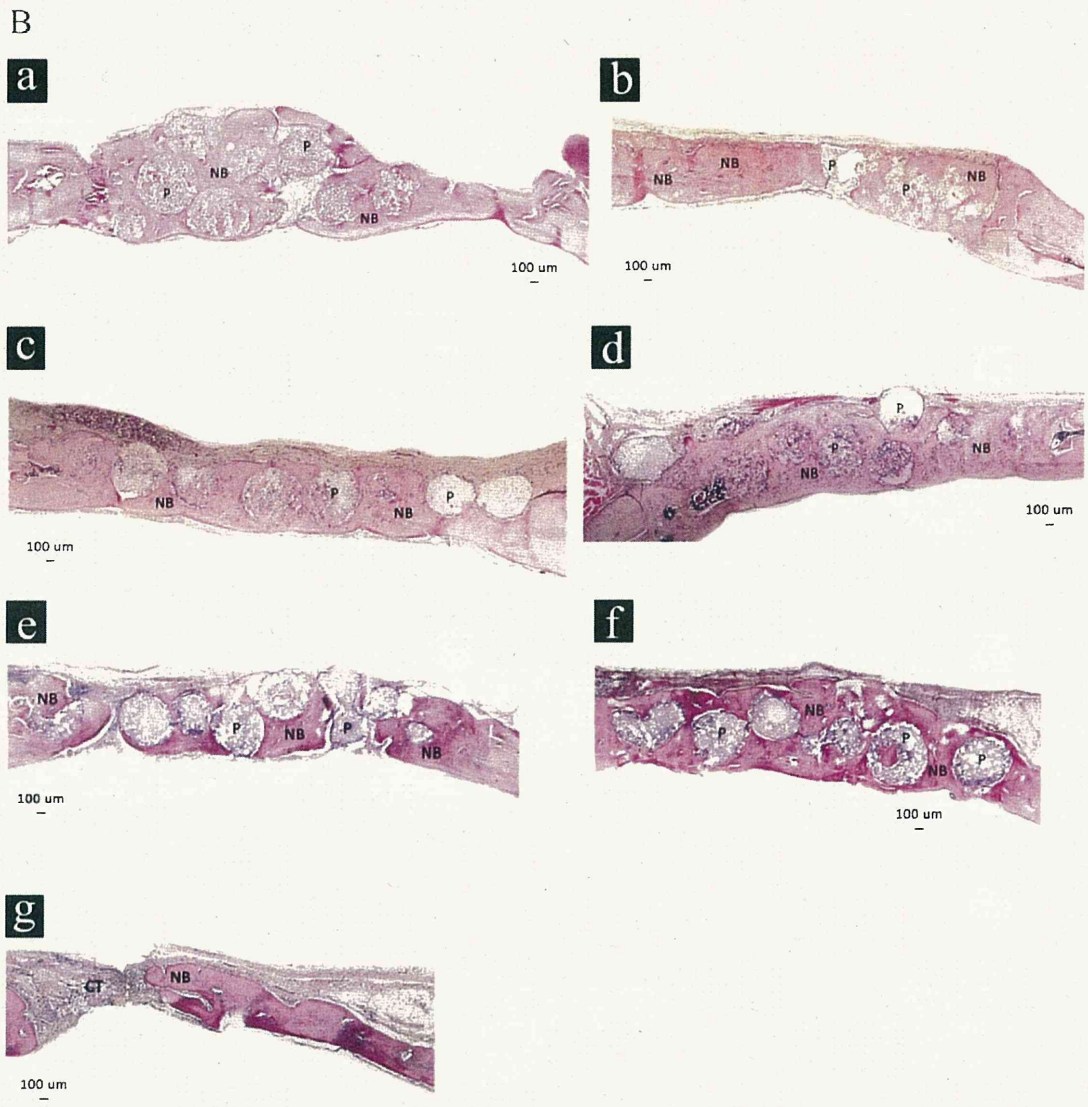

FIGURE 2. Continued

Statistical analysis

For the numerical data gathered, statistical analysis was performed by commercial software (SPSS) with One-way analysis of variance (ANOVA), where results suggested a significant difference between groups ($p < 0.05$). The data were further analyzed by *Tukey's post hoc* multiple comparisons test.

RESULTS

Macroscopic observation

During the recovery phase, no macroscopic infection of the wound was noted. However, all simvastatin groups showed a reddish inflammation in the skin area overlying the bone defects, the inflammation was subsided to a normal skin within 10 days. The wounds showed a complete healing after 2 weeks.

Histological observation

The histological images are presented in Figures 2–4.

Control groups

In both 6 and 8 weeks, the new bone failed to progress toward the center of the defect and only a thin layer of new bone was seen at the defect margins. The central portion of defect was filled with compressed fibrous connective tissue [Fig. 2(A-g,B-g)].

α-TCP groups

In 6 weeks group, the defects were filled with new bone islands between the particles with the presence of woven bone. The particles are starting to degrade and partially replaced by new bone [Fig. 2(A-a)]. In 8 weeks group, more bone was taking place of the degraded particles, and there was more bone formation in between the particles [Fig. 2(B-a)].

In 6 weeks with simvastatin group, the defects were not completely filed with bone, the particles were ongoing

degradation and replaced mostly by woven bone [Fig. 2(A-b)]. In 8 weeks with simvastatin group, the new bone filled the defect almost completely, and the particles are also mostly replaced by new bone [Fig. 2(B-b)].

β-TCP groups

In 6 weeks group, new bone took place in parts of the defect with presence of woven bone and some connective tissue, the particles were slightly degraded [Fig. 2(A-c)]. In 8 weeks group, the new bone was occupying most of the defects, and the particles were further degraded [Fig. 2(B-c)].

In 6 weeks with simvastatin group, the new bone took place in more parts of the defect in comparison with the non simvastatin group, and the particles are also slightly degraded [Fig. 2(A-d)]. In 8 weeks with simvastatin group, the new bone was filling the defects almost completely, and the particles were further degraded and replaced by new bone [Fig. 2(B-d)].

HA groups

In 6 weeks, the new bone took place at the margins of the defects, woven bone was filling the center of the defects and spaces between particles, the particles showed no degradation [Fig. 2(A-e)]. In 8 weeks, the new bone was filling the spaces between particles, and the particles showed least degradation [Fig. 2(B-e)].

In 6 weeks simvastatin group, parts of the defects were filled with new bone while other parts were filled with woven bone, and the particles showed no degradation [Fig. 2(B-f)]. In 8 weeks with simvastatin group, more bone was filling the defects in comparison with the non simvastatin group, and particle also showed least degradation [Fig. 2(B-f)].

As shown in Figure 3, the group of HA with simvastatin showed significant increase in number of osteoblastic cells compared with the group without simvastatin, which was also evident in the groups of α-TCP and β-TCP with/without simvastatin. The pattern of bone formation suggests that the osteoblastic cells were differentiated from the dura mater.

Degradation of the materials

There was a significant difference in the degradability of the three bone substitute materials. As for the α-TCP particles almost all the particles had degraded after 8 weeks, while β-TCP showed degradation to some extent but significantly less than α-TCP. HA particles showed least amount of degradation and can be clearly observed (Fig. 4).

Radiological findings

Control groups. In both 6 and 8 weeks showed scanty amount of thin bone extending toward the center but failed to fill the defect [Fig. 5(A-g,B-g)].

α-TCP groups. In 6 and 8 weeks particles were reduced in size, less radio opaque and well integrated with significant amount of new bone [Fig. 5(A-a,B-a)]. Simvastatin groups were showing more amount of new bone and the opacity of the particles is almost similar to the bone which can be clearly observed in α-TCP + statin 8 weeks group [Fig. 5(A-b,B-b)].

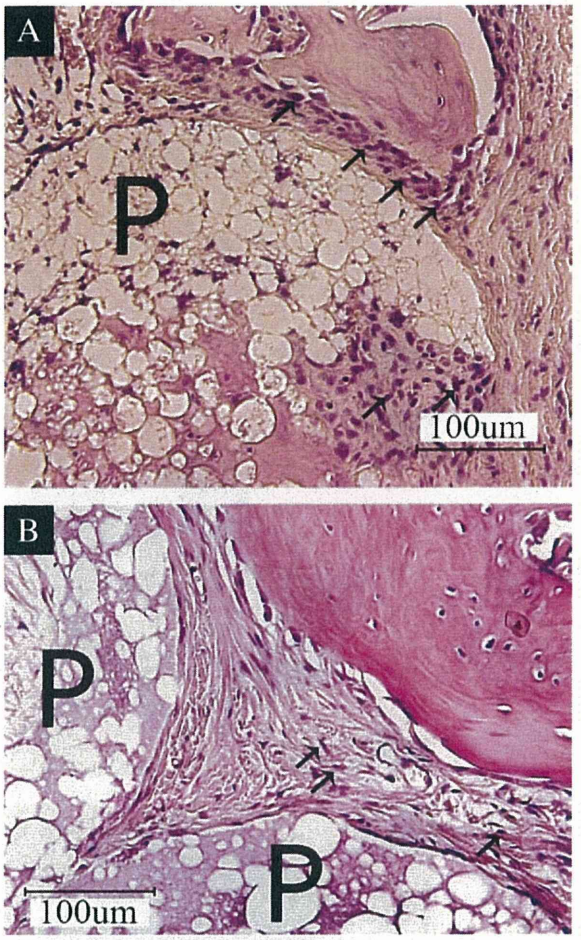

FIGURE 3. Higher magnified histological images of HA group with simvastatin (A) and without simvastatin (B) at 6 weeks. Bone substitute particles (P) and osteoblastic cells (arrows). [Color figure can be viewed in the online issue, which is available at wileyonlinelibrary.com.]

β-TCP groups. At 6 weeks, newly formed bone and β-TCP particles could be easily differentiated as they revealed different radiopacity [Fig. 5(A-c)], in simvastatin group more bone is observed [Fig. 5(A-d)]. At 8 weeks, particles are slightly reduced in size and more new bone can be observed, in simvastatin group no difference in particles size can be seen but more new bone is formed [Fig. 5(B-c,B-d)].

HA groups. At 6 and 8 weeks particles showed least reduction in size for both non simvastatin and simvastatin groups [Fig. 5(A-e,f,B-e,f)]. Bone formation was scattered between the particles in 6 weeks group [Fig. 5(A-e)], but it appears to fill in between particles in statin group [Fig. 5(A-f)]. In 8 weeks, statin group showed higher amount of new bone than non- statin group [Fig. 5(B-e,f)].

DISCUSSION

Although autologous graft is the golden standard for the graft materials,[17,18] it is not always possible to harvest sufficient amount of bone due to factors such as the limitation

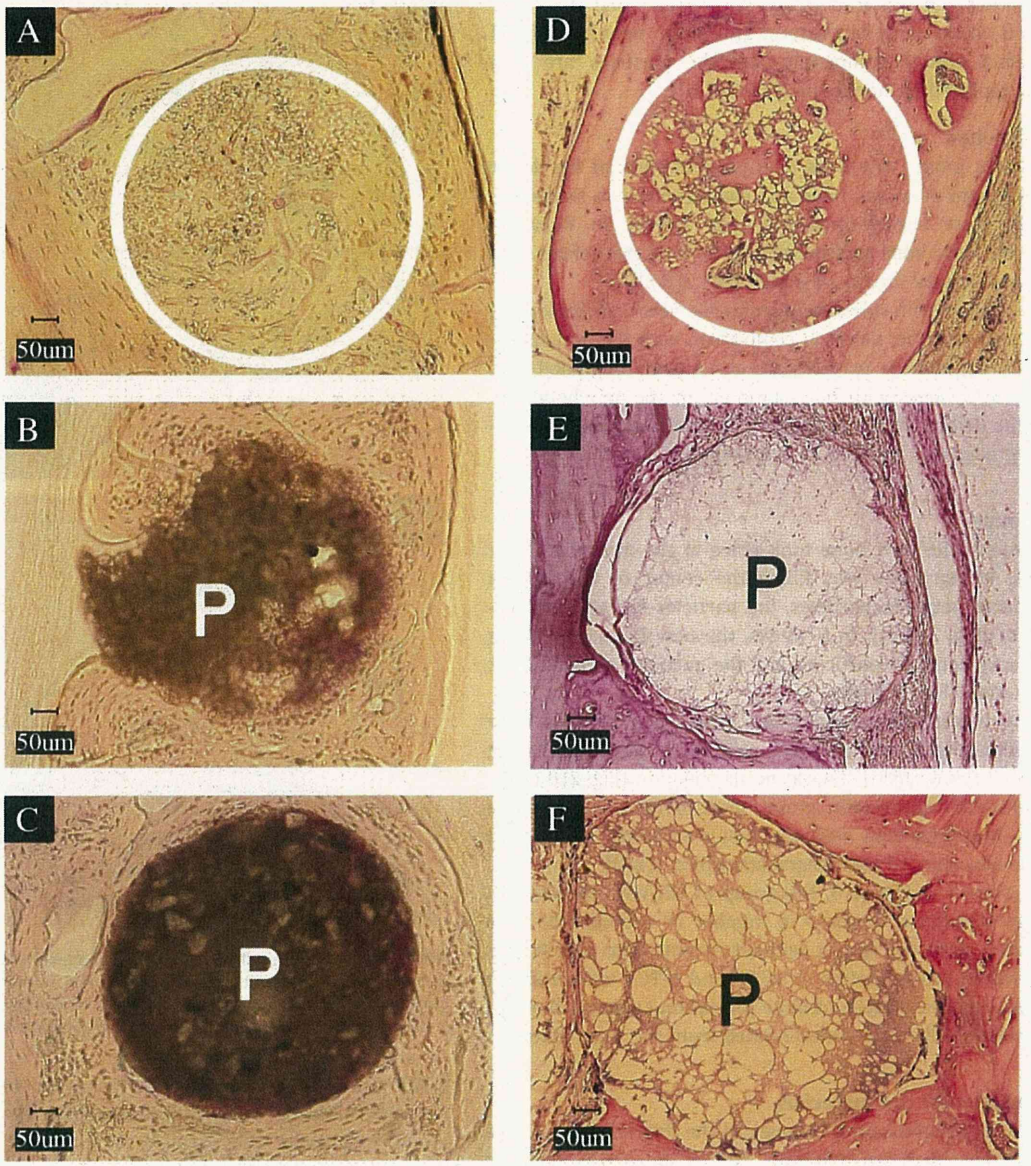

FIGURE 4. Histological images representing degradability between the three types of bone substitutes at 8 weeks. α-TCP particles are the most degraded (A,D), followed by β-TCP (B,E), while HA particles are the least degraded and can be clearly seen (C,F). Circles in (A,D) indicates the area of the degraded particles. α-TCP (A), β-TCP (B), HA (C) (Villanueva bone stain), α-TCP (D), β-TCP (E), HA (F) (H&E stain). [Color figure can be viewed in the online issue, which is available at wileyonlinelibrary.com.]

of donor sites.[19–21] Therefore many researchers have investigated calcium phosphate as bone graft material because of its good biocompatibility,[12,22] it was introduced successfully as a bone substitute material. Although bone substitutes currently available are osteoconductive, more effective material is clinically desired. In this study, the osteoconductivity of three different bone substitute materials was evaluated in bilateral rat calvarial model. In Figure 6(A,B) the quantitative results show the percentage of new bone formation among 6 and 8 weeks groups. In α-TCP + statin group, the percentage was the highest compared with the other bone substitute materials, while in control group the percentage was the lowest. Furthermore, the percentage was significantly higher within the same material when simvastatin was added in both α-TCP and β-TCP groups, while no significance was found in the HA group, however the percentage has a tendency to increase when simvastatin was added to HA particles. Accordingly, the results of this study suggest that TCP was better osteoconductive than HA and this can be attributed to the biodegradability of the TCP which led into significance in the results. Despite the degradability of α-TCP over β-TCP, there was no significant difference in the percentage of new bone formed among these two TCP materials [Fig. 6(A,B)]. The rate of bone formation versus particle

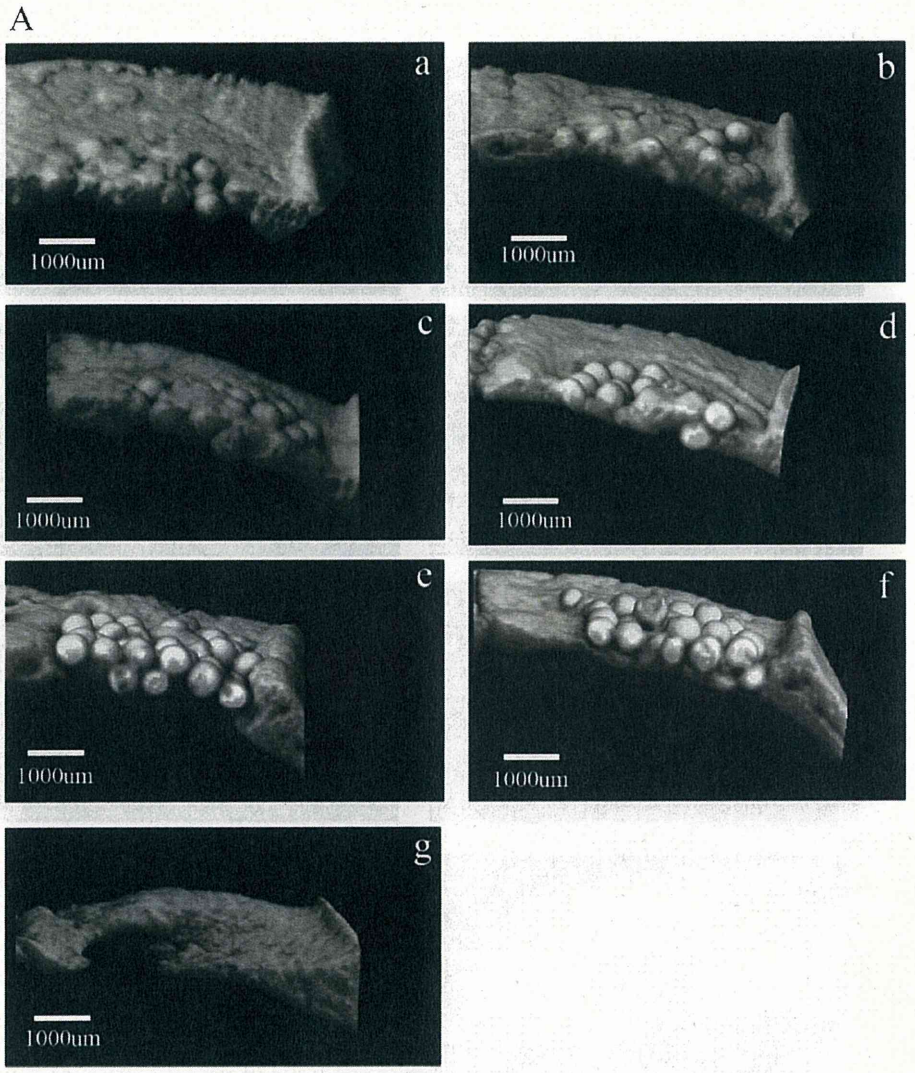

FIGURE 5. (A) Micro CT images for cross section in the coronal plane of the calvarial bone at 6 weeks, slightly tilted to show the region of interest. The bone failed to fill the center of the defect in control group (g). Note that α-TCP (Alpha tricalcium phosphate) particles are less radio opaque (a,b) when compared with the other two types. α-TCP (a), α-TCP + statin (b), β-TCP (c), β-TCP + statin (d), HA (e), HA + statin (f), and Control (g). (B) Micro CT images for cross section in the coronal plane of the calvarial bone at 8 weeks, slightly tilted to show the region of interest. α-TCP (a), α-TCP + statin (b), β-TCP (c), β-TCP + statin (d), HA (e), HA + statin (f), and Control (g).

degradation is an important factor. Therefore, the ideal bone substitute material can be defined as the one that degrades in synchronous manner with the bone formation. It has been reported that the ideal graft substitute should reabsorb with time to allow and encourage new bone formation whilst maintaining its properties as an osteoconductive scaffold until it is no longer required.[23] In this study, quantitative results of the remaining bone substitute materials demonstrated that after 6 and 8 weeks, less than 10% of α-TCP particles remained [Fig. 7(A,B)]. Consequently, this study suggests that α-TCP is the material of choice among the tested substitutes due to the higher degradability rate which may provide sufficient space for bone formation. However, based on histological observation and quantitative analysis it was noticed that the degradation rate of α-TCP is slightly higher than the bone formation rate [Fig. 4(A,D)], but it was within the acceptable rate, as α-TCP successfully acted as a space maintainer, scaffold, and osteoconductive material.

Simvastatin is an inhibitor of cholesterol synthesis that has the effect of stimulating bone formation.[16,24,25] Previous studies showed that it stimulates the BMP-2 expression in osteoblasts and that it also inhibits the osteoclastic activity.[26–29] Thus, it is reasonable to expect that combining a bone substitute with simvastatin favorably modifies the material character by stimulating bone formation. In this study, the highest BMC and BMD in 6 and 8 weeks were found when combining simvastatin with α-TCP (Tables II and III). The simvastatin dose in this study was determined

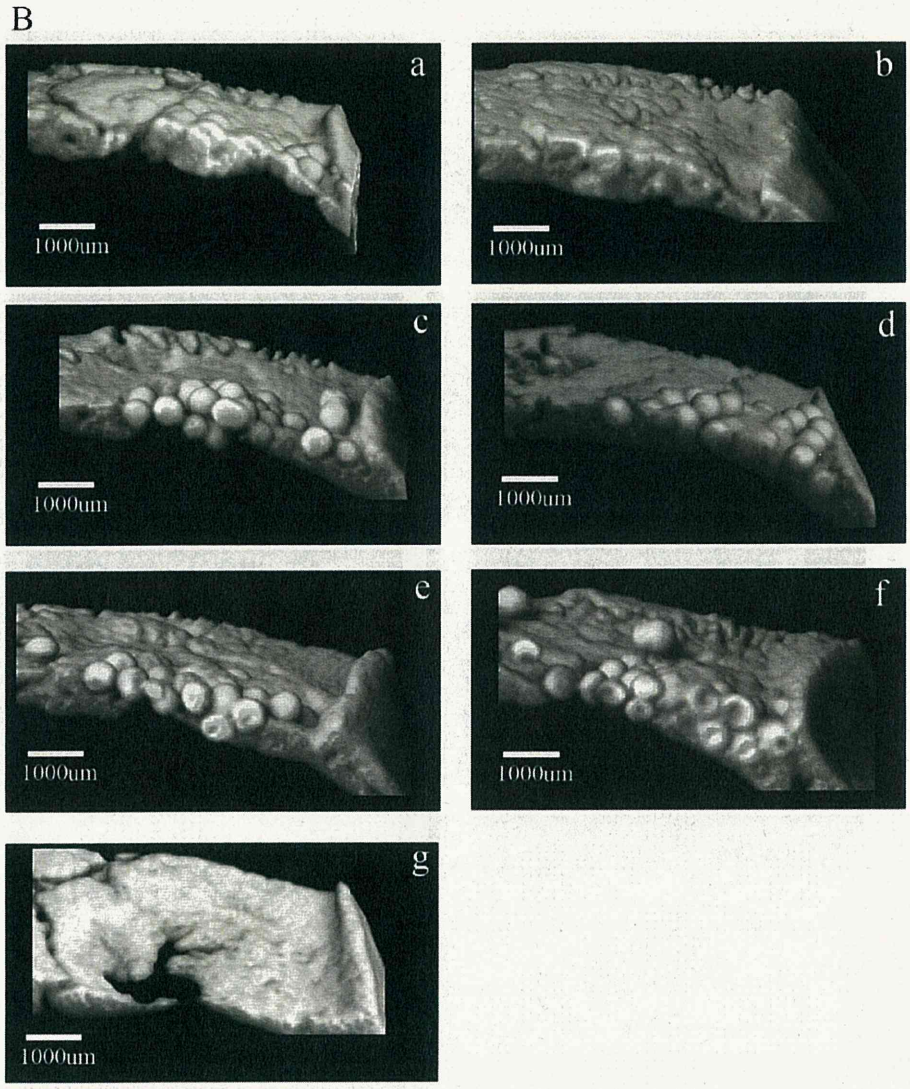

FIGURE 5. Continued

according to our previous study that showed that optimum dose for the same defect sizes was 0.1 mg. In the previous study, a higher dose led to inflammation of the skin above the defects while lower dose did not stimulate bone formation.[30] However, in this study, skin inflammation was observed over the applied area although this inflammation was slight and temporal. The releasing mechanism of the simvastatin from the materials is not clear. The drug release from the material would be affected by the solubility of the drug in the surrounding solution, the binding strength of the drug to the material, the material porosity and the material degradation speed. Our previous *in vitro* study demonstrated that more than half of the simvastatin was released from α-TCP particles on the first day, which was followed by slow release of the drug.[26] The releasing profile of the drug from the three materials *in vivo* is different because the degradation rate of the materials strongly affects the drug release. However, it is likely that the initial burst of drug release from the materials also occurred *in vivo* in this study. It would be much beneficial to control the release of the simvastatin on the basis of a daily dose,[31] this could secure a sustained stimulation of the bone formation for appropriate period of time.

In our previous study, combining α-TCP with simvastatin stimulated MAR compared with the one of α-TCP alone. However, in this study, the MAR was not stimulated when the materials were combined with simvastatin at the same dose (Tables II and III). This is probably due to the difference of the time points of the histomorphometrical measurement: 4 and 6 weeks in the previous study; 6 and 8 weeks in this study due to that the most of the simvastatin has been released at an earlier time. Furthermore, it would be also possible that there were differences in the microstructure and/or crystal size between the previous

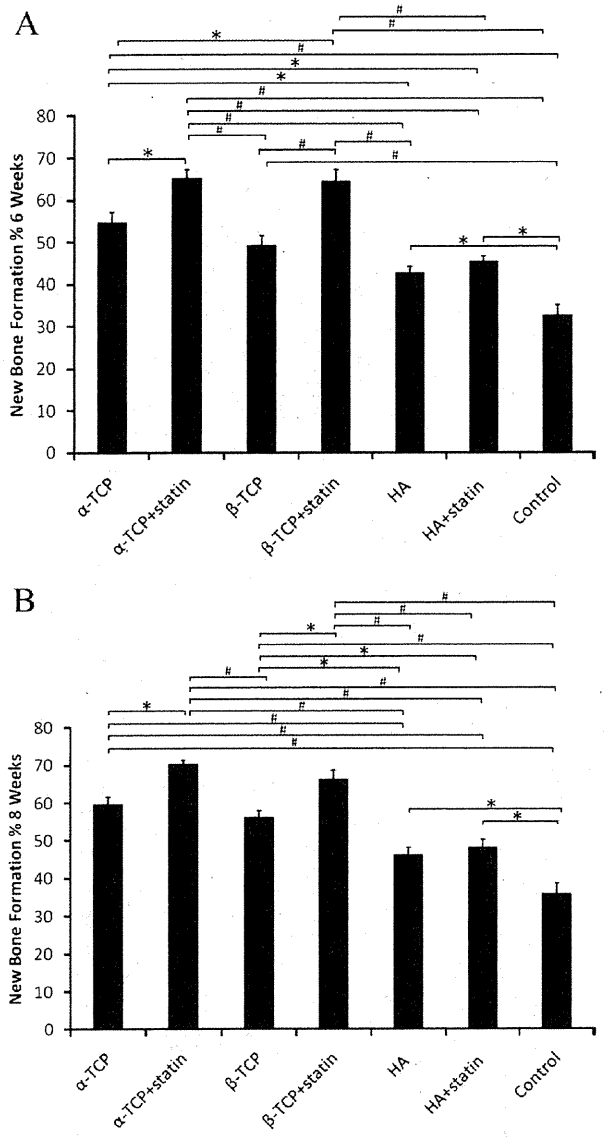

FIGURE 6. (A) Percentage of new bone formation in 6 weeks. $^{*}p \leq 0.05$, $^{\#}p < 0.001$. Values are shown as mean ± SEM. The highest percentage of new bone formation was found in α-TCP with statin group. Statin had a significant role in new bone formation among the two TCP bone substitutes, however, no significance was observed when using statin in HA particles. (B) Percentage of new bone formation in 8 weeks. $^{*}p \leq 0.05$, $^{\#}p < 0.001$. Values are shown as mean ± SEM. The percentage of new bone formation was slightly increased compared with 6 weeks.

and the present materials, which affected the releasing speed of the drug from the materials. The temporal inflammatory response of the skin on the applied area in this study, which was not observed in the previous study, could be probably explained by higher rate of drug release from the materials in this study compared with the previous study.

The pattern of bone formation suggests that the osteoprogenitor cells are differentiated from the dura mater. The number of osteoblast cells was significantly higher in the simvastatin groups compared with non simvastatin groups. This can be attributed to the role of simvastatin in stimulating BMP-2 which is a family member of the Transforming growth factor beta protein (TGF-β) that controls proliferation, and cellular differentiation.[32–35]

The defect size used in this study was 5 mm in diameter, which can be considered critical as new bone formation in most defects failed to fill the center after 8 weeks in the control group. The bone substitute particles size used in this study was about 500–750 μm, the particle size was found to influence the outcome of the bone formation process.[36,37] However, in this study, we standardized the size and the microstructure of the three materials to eliminate the potential effect of these factors on bone formation.

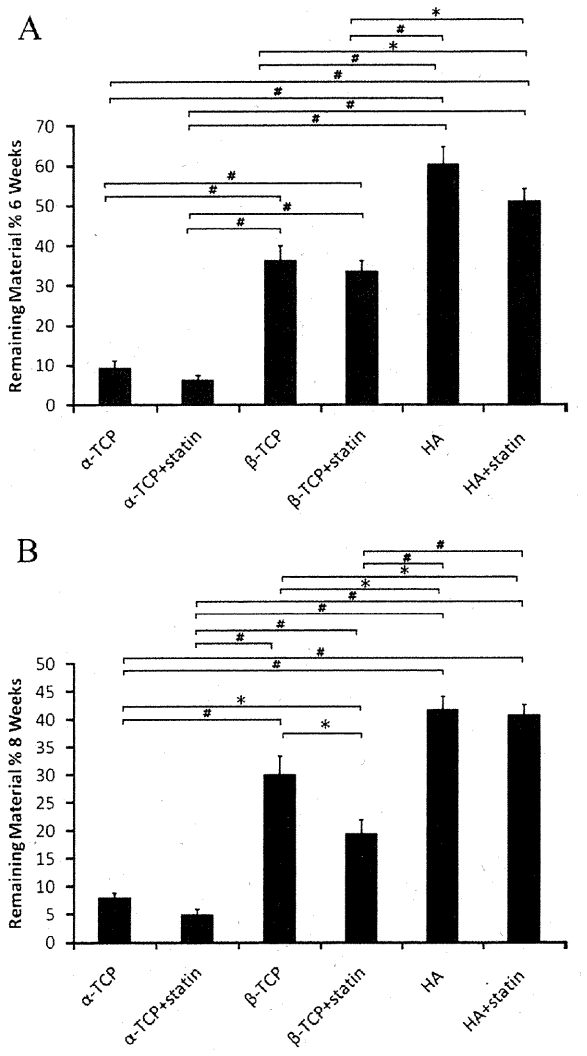

FIGURE 7. (A) Percentage of remaining material in 6 weeks. $^{*}p \leq 0.05$, $^{\#}p < 0.001$. Values are shown as mean ± SEM. The degraded α-TCP particles are significantly higher than the other two bone substitute materials which may potentially create room for more bone formation. (B) Percentage of remaining material in 8 weeks. $^{*}p \leq 0.05$, $^{\#}p < 0.001$. Values are shown as mean ± SEM. Interestingly, the combination of the bone substitute materials with simvastatin affected the degradation of the materials.

TABLE II. Mineral Apposition Rate (MAR), Bone Mineral Contents (BMC), and Bone Mineral Density (BMD) in 6 Weeks

Experimental Group	MAR (μm)	BMC (mg)	BMD (mg/mm^3)
α-TCP	4.32 ± 0.24	13.04 ± 1.05	1.06 ± 0.02
α-TCP+statin	5.20 ± 0.55	13.79 ± 0.79	1.26 ± 0.02
β-TCP	3.14 ± 0.33	10.90 ± 0.46	1.04 ± 0.01
β-TCP+statin	3.44 ± 0.44	12.08 ± 0.42	1.16 ± 0.007
HA	2.67 ± 0.20	10.80 ± 0.39	1.02 ± 0.01
HA+statin	3.1 ± 0.10	11.51 ± 0.45	1.10 ± 0.02
Control	2.16 ± 0.24	8.21 ± 0.04	0.97 ± 0.009

One-way ANOVA with Tukey's post-hoc multiple comparison: $^*p \leq 0.05$, $^\#p < 0.001$. Values are shown as mean ± SEM.

TABLE III. Mineral Apposition Rate (MAR), Bone Mineral Contents (BMC), and Bone Mineral Density (BMD) in 8 Weeks

Experimental Group	MAR (μm)	BMC (mg)	BMD (mg/mm^3)
α-TCP	2.68 ± 0.42	13.13 ± 0.33	1.25 ± 0.01
α-TCP+statin	3.65 ± 0.14	15.26 ± 0.67	1.30 ± 0.02
β-TCP	2.79 ± 0.11	13.33 ± 0.74	1.21 ± 0.01
β-TCP+statin	2.91 ± 0.26	14.45 ± 1.05	1.23 ± 0.01
HA	1.91 ± 0.18	12.53 ± 0.70	1.19 ± 0.008
HA+statin	2.22 ± 0.16	13.36 ± 0.53	1.21 ± 0.016
Control	1.38 ± 0.05	8.91 ± 0.71	1.12 ± 0.009

One-way ANOVA with Tukey's post-hoc multiple comparison: $^*p \leq 0.05$, $^\#p < 0.001$. Values are shown as mean ± SEM.

This study confirmed the difference in the order of degradability of the three materials; α-TCP is the most degradable followed by β-TCP, and HA is the least degradable [Figs. 4 and 7(A,B)]. Interestingly, the combination of the bone substitute materials with simvastatin affected not only bone formation but also the material degradation. Degradation of α-TCP and β-TCP is affected by the solubility of these materials. In addition, it is possible that the degradation of these materials is strongly affected by the bone remodeling speed around the materials, which could explain the more degradation of α-TCP and β-TCP in the simvastatin groups.

CONCLUSION

This study confirmed that α-TCP, β-TCP, and HA are osteoconductive materials acting as space maintainer for bone formation when applied to a bone defect, and demonstrated that combining these materials with simvastatin stimulates bone regeneration and it also affects degradability of α-TCP and β-TCP. Conclusively, α-TCP has the advantage of higher rate of degradation allowing the more bone formation and combining α-TCP with simvastatin enhances this property.

REFERENCES

1. John HD, Wenz B. Histomorphometric analysis of natural bone mineral for maxillary sinus augmentation. Int J Oral Maxillofac Implants 2004;19:199–207.
2. Boyne PJ, James RA. Grafting of the maxillary sinus floor with autogenous marrow and bone. J Oral Surg 1980;38:613–616.
3. Brugnami F, Caiazzo A, Leone C. Local intraoral autologous bone harvesting for dental implant treatment: Alternative sources and criteria of choice. Keio J Med 2009;58:24–28.
4. Moy PK, Lundgren S, Holmes RE. Maxillary sinus augmentation: Histomorphometric analysis of graft materials for maxillary sinus floor augmentation. J Oral Maxillofac Surg 1993;51:857–862.
5. Younger EM, Chapman MW. Morbidity at bone graft donor sites. J Orthop Trauma 1989;3:192–195.
6. Yuan H, Yang Z, De Bruij JD, De Groot K, Zhang X. Material-dependent bone induction by calcium phosphate ceramics: A 2.5-year study in dog. Biomaterials 2001;22:2617–2623.
7. Kasugai S. Local application of statin for bone augmentation. Clin Calcium 2005;15:67–72.
8. Kasugai S, Fujisawa R, Waki Y, Miyamoto K, Ohya K. Selective drug delivery system to bone: Small peptide (Asp)6 conjugation. J Bone Miner Res 2000;15:936–43.
9. Li F, Zhao X, Wu J. Repair of bone defect with allograft demineralized bone containing basic fibroblast growth factor in rabbits. Zhongguo Xiu Fu Chong Jian Wai Ke Za Zhi 2005;19:431–434.
10. Santos FA, Pochapski MT, Martins MC, Zenobio EG, Spolidoro LC, Marcantonio E. Comparison of biomaterial implants in the dental socket: Histological analysis in dogs. Clin Implant Dent Relat Res 2010;12:18–25.
11. Smeets R, Grosjean MB, Jelitte G, Heiland M, Kasaj A, Riediger D, Yildirim M, Spiekermann H, Maciejewski O. Hydroxyapatite bone substitute (Ostim) in sinus floor elevation. Maxillary sinus floor augmentation: Bone regeneration by means of a nanocrystalline in-phase hydroxyapatite (Ostim). Schweiz Monatsschr Zahnmed 2008;118:203–212.
12. Alcaide M, Serrano MC, Pagani R, Sanchez-Salcedo S, Vallet-Regi M, Portoles MT. Biocompatibility markers for the study of interactions between osteoblasts and composite biomaterials. Biomaterials 2009;30:45–51.
13. Kihara H, Shiota M, Yamashita Y, Kasugai S. Biodegradation process of alpha-TCP particles and new bone formation in a rabbit cranial defect model. J Biomed Mater Res B Appl Biomater 2006;79:284–291.
14. Yamaguchi K, Hirano T, Yoshida G, Iwasaki K. Degradation-resistant character of synthetic hydroxyapatite blocks filled in bone defects. Biomaterials 1995;16:983–985.
15. Mundy G, Garrett R, Harris S, Chan J, Chen D, Rossini G, Boyce B, Zhao M, Gutierrez G. Stimulation of bone formation in vitro and in rodents by statins. Science 1999;286:1946–1949.
16. Nyan M, Sato D, Oda M, Machida T, Kobayashi H, Nakamura T, Kasugai S. Bone formation with the combination of simvastatin and calcium sulfate in critical-sized rat calvarial defect. J Pharmacol Sci 2007;104:384–386.
17. Giannoudis PV, Dinopoulos H, Tsiridis E. Bone substitutes: An update. Injury 2005;36(Suppl 3):S20–S27.
18. Rueger JM. Bone substitution materials. Current status and prospects. Orthopade 1998;27:72–79.
19. Baqain ZH, Anabtawi M, Karaky AA, Malkawi Z. Morbidity from anterior iliac crest bone harvesting for secondary alveolar bone grafting: An outcome assessment study. J Oral Maxillofac Surg 2009;67:570–575.
20. Beirne JC, Barry HJ, Brady FA, Morris VB. Donor site morbidity of the anterior iliac crest following cancellous bone harvest. Int J Oral Maxillofac Surg 1996;25:268–271.
21. Swan MC, Goodacre TEE. Morbidity at the iliac crest donor site following bone grafting of the cleft alveolus. Br J Oral Maxillofac Surg 2006;44:129–133.
22. Yoshimine Y, Akamine A, Mukai M, Maeda K, Matsukura M, Kimura Y, Makishima T. Biocompatibility of tetracalcium phosphate cement when used as a bone substitute. Biomaterials 1993;14:403–406.
23. Walsh WR, Vizesi F, Michael D, Auld J, Langdown A, Oliver R, Yu Y, Irie H, Bruce W. Beta-TCP bone graft substitutes in a bilateral rabbit tibial defect model. Biomaterials 2008;29:266–271.
24. Mundy G, Garrett R, Harris S, Chan J, Chen D, Rossini G, Boyce B, Zhao M, Gutierrez G. Stimulation of bone formation in vitro and in rodents by statins. Science 1999;286:1946–1949.
25. Stein D, Lee Y, Schmid MJ, Killpack B, Genrich MA, Narayana N, Marx DB, Cullen DM, Reinhardt RA. Local simvastatin effects on mandibular bone growth and inflammation. J Periodontol 2005; 76:1861–1870.
26. Nyan M, Miyahara T, Noritake K, Hao J, Rodriguez R, Kuroda S, Kasugai S. Molecular and tissue responses in the healing of rat calvarial defects after local application of simvastatin combined with alpha tricalcium phosphate. J Biomed Mater Res B Appl Biomater 2010;93:65–73.
27. Boyne PJ, Salina S, Nakamura A, Audia F, Shabahang S. Bone regeneration using rhBMP-2 induction in hemimandibulectomy type defects of elderly sub-human primates. Cell Tissue Bank 2006;7:1–10.
28. Duan Z, Zheng Q, Guo X, Li C, Wu B, Wu W. Repair of rabbit femoral defects with a novel BMP2-derived oligopeptide P24. J Huazhong Univ Sci Technol Med Sci 2008;28:426–430.
29. Giannoudis PV. Fracture healing and bone regeneration: Autologous bone grafting or BMPs? Injury 2009;40:1243–1244.
30. Nyan M, Sato D, Kihara H, Machida T, Ohya K, Kasugai S. Effects of the combination with alpha-tricalcium phosphate and simvastatin on bone regeneration. Clin Oral Implants Res 2009;20:280–287.
31. Skoglund B, Aspenberg P. Locally applied Simvastatin improves fracture healing in mice. BMC Musculoskelet Disord 2007;8:98.
32. Hatano H, Maruo A, Bolander ME, Sarkar G. Statin stimulates bone morphogenetic protein-2, aggrecan, and type 2 collagen gene expression and proteoglycan synthesis in rat chondrocytes. J Orthop Sci 2003;8:842–848.
33. Sonobe M, Hattori K, Tomita N, Yoshikawa T, Aoki H, Takakura Y, Suguro T. Stimulatory effects of statins on bone marrow-derived mesenchymal stem cells. Study of a new therapeutic agent for fracture. Biomed Mater Eng 2005;15:261–267.
34. Zhang H, Lin C-Y. Simvastatin stimulates chondrogenic phenotype of intervertebral disc cells partially through BMP-2 pathway. Spine (Phila Pa 1976) 2008;33:525–531.
35. Zhang M, Li XP, Qiao Y, Nie SP, Ma CS. Does treatment with statins have the potential of enhancing vascular calcification? Chin Med J (Engl) 2008;121:473–474.
36. Mankani MH, Kuznetsov SA, Fowler B, Kingman A, Robey PG. In vivo bone formation by human bone marrow stromal cells: Effect of carrier particle size and shape. Biotechnol Bioeng 2001;72:96–107.
37. Sun JS, Tsuang YH, Chang WH, Li J, Liu HC, Lin FH. Effect of hydroxyapatite particle size on myoblasts and fibroblasts. Biomaterials 1997;18:683–690.

Magnitude and Direction of Mechanical Stress at the Osseointegrated Interface of the Microthread Implant

Malik I. Hudieb,*† Noriyuki Wakabayashi,‡ and Shohei Kasugai*†

Background: The mechanism by which the microthread implant preserves peri-implant crestal bone is not known. The objective of this research is to assess the effect of microthreads on the magnitude and direction of the stress at the bone–implant interface using finite element analysis modeling.

Methods: Three-dimensional finite element models representing the microthreaded implant (microthread model) and smooth surface implant (smooth model) installed in the mandibular premolar region were created based on microscopic and computed tomography images. The mesh size was determined based on convergence tests. Average maximum bite force of adults was used with four loading angles on the occlusal surface of the prosthesis.

Results: Regardless of the loading angle, principal stresses at the bone–implant interface of the microthread model were always perpendicular to the lower flank of each microthread. In the smooth model, stresses were affected by the loading angle and directed obliquely to the smooth interface, resulting in higher shear stress. The interfacial stresses decreased gradually in the apical direction in both models but with wavy pattern in the microthread model and smooth curve for the smooth model. Although peak principal stress values were higher around the microthread implant, peri-implant bone volume exhibiting a high strain level >4,000 μ was smaller around the microthread implant compared to the smooth implant.

Conclusion: Stress-transferring mechanism at the bone–implant interface characterized by the direction and profile of interfacial stresses, which leads to more compressive and less shear stress, may clarify the biomechanical aspect of microthread dental implants. *J Periodontol 2011;82:1061-1070.*

KEY WORDS

Bone and bones; dental implant; finite element analysis; occlusal force; stress, mechanical.

* Department of Oral Implantology and Regenerative Dental Medicine, Graduate School, Tokyo Medical and Dental University, Tokyo, Japan.
† Global Center of Excellence Program "International Research Center for Molecular Science in Tooth and Bone Diseases," Tokyo Medical and Dental University.
‡ Department of Removable Prosthodontics, Division of Oral Health Sciences, Graduate School, Tokyo Medical and Dental University.

Microthread structure has been proposed as a bone-retention element at the implant neck to stabilize the peri-implant marginal bone level.[1] Animal experiments have demonstrated larger mineralized bone that comes in contact with implant surface and well-maintained marginal bone levels around microthread implants.[2-4] In clinical studies, radiographic evaluation revealed insignificant amounts of crestal bone loss around microthread implants up to 5 years follow-up.[5-7]

The benefit of microthreads, however, has not been well understood from the mechanical viewpoint. Controversy began with a two-dimensional finite element (FE) study[8] that indicated that the microthread implant had 29% greater maximum von Mises stress at the crestal bone adjacent to the implant than a smooth-neck implant. Opposition was posted to make clarification on some questions regarding the condition at the bone–implant interface, reliability of the material properties, and precision of the modeling.[9] What makes these communications an insoluble issue may partially result from the current lack of knowledge about how mechanical stimulations in terms of stress and strain affect bone retention around implants.

In addition, the contribution of occlusal loads in the pathogenesis of peri-implant marginal bone loss has not been sufficiently verified. Occlusal conditions and overloading have often been proposed

doi: 10.1902/jop.2010.100237